EI SEVIER

Contents lists available at ScienceDirect

Optics Communications

journal homepage: www.elsevier.com/locate/optcom



Dynamic control of a phase-shifted FBG through acousto-optic modulation

C.A.F. Marques ^{a,*}, R.A. Oliveira ^{b,c}, A.A.P. Pohl ^b, J. Canning ^c, R.N. Nogueira ^{a,d}

- ^a Instituto de Telecomunicações, Pólo de Aveiro, 3810-193 Aveiro, Portugal
- ^b Federal University of Technology, Parana, Av. Sete de Setembro, 3165, Curitiba, PR, CEP 80230-901, Brazil
- ^c Interdisciplinary Photonics Laboratories (iPL), University of Sydney, The School of Chemistry, F09, Camperdown, Sydney, NSW 2006, Australia
- ^d Nokia Siemens Networks Portugal S.A., 2720-093, Portugal

ARTICLE INFO

Article history:
Received 2 June 2010
Received in revised form 20 October 2010
Accepted 9 November 2010

Keywords:
Acousto-optic modulation (AOM)
Phase-shifted fiber Bragg grating (PSFBG)
Acoustic wave

ABSTRACT

When an acoustic wave excites a phase-shifted fiber Bragg grating (PSFBG) several properties of the transmission/reflection spectrum, such as transmission notch depth and spectral bandwidth are influenced. In this work, a study on the effect of acoustic waves in PSFBGs is presented. The results are supported by theoretical simulation and experimental work. The technique can be used for different applications, such as in a fast tunable optical notch filter.

© 2010 Elsevier B.V. All rights reserved.

1. Introduction

Fiber Bragg grating (FBG) as a compact in-line optical fiber filter has attracted much interest and has been the key for important all-fiber devices [1]. The significant development of FBG technology has ultimately contributed to lowering the costs of systems employed in optical communications. One weakness associated with FBG technology is the difficulty to develop fast tunable devices. The tuning methods presented so far based on strain [2] or temperature [3] are slow and bulky, with tuning times of milliseconds. This drawback has been partially overcome using acousto-optic modulation (AOM), whose tuning time is of the order of a few microseconds. This effect has been successfully applied in the design and construction of various low insertion loss all-fiber devices, such as modulators [4], tunable notch filter [5], switchable comb filters [6], Q-switched fiber lasers [7], fast add-drop multiplexer [8] among others. These devices have already been the target of an optimization and a thorough analysis in terms of optical spectral domain and vibrational modes [9-11]. When an acoustic wave is coupled into a fiber where an FBG is inscribed it generates a standing mechanical wave [11]. However, depending on its frequency, it generates bends in the fiber, that causes a reduction in the FBG reflectivity (flexural regime), or compression and rarefaction zones, so creating additional bands to appear on both sides of the grating reflection spectrum (longitudinal regime) [10–12].

The need to tailor the transmission FBG spectrum to obtain very narrow stop bands has led to the introduction of a phase shift across the

2. Numerical simulation

A PSFBG is characterized by the introduction of a phase-shift across the grating reflection spectrum. The key characteristic of such a device is the existence of transmission windows at the FBG reflection band, resulting in high wavelength selectivity. The simulation of the PSFBG spectrum can be accomplished using the transfer matrix method (TMM) [17]. By discretizing the grating in M uniform sections described by 2×2 matrices (F_i) and defining R_i and S_i as the reflection and the transmission coefficients of the fields across one section i, the resulting coefficients after the signal has passed through M transverse sections are calculated as

$$\begin{bmatrix} R_{M} \\ S_{M} \end{bmatrix} = F_{M} \cdot F_{M-1} \cdot \dots \cdot F_{i} \cdot \dots \cdot F_{1} \begin{bmatrix} R_{0} \\ S_{0} \end{bmatrix}. \tag{1}$$

grating. The principle of phase shifts was first demonstrated in periodic structures made from semiconductor materials [13]. Techniques were then developed to produce phase-shifts in fiber gratings [14,15]. More recently, the control of phase shifts by acoustic waves has gained attention as a means of controlling the Q-switching in DFB fiber lasers [7,16]. In this work we present detailed results on the characteristics of uniform phase-shifted fiber Bragg gratings (PSFBG) under the excitation of acoustical waves. Weak PSFBGs are used to ensure sufficient resolution of the phase shift so that the phenomenological changes are readily observed on an optical spectrum analyzer without the use of other higher resolution methods required to properly characterize strong phase-shifted gratings. It is also demonstrated that for higher acoustic frequencies, when longitudinal waves are excited, the sampling modulation of the grating is achieved with the generation of multiple peaks.

^{*} Corresponding author. E-mail address: cmarques@av.it.pt (C.A.F. Marques).

The matrix representing the phase-shift is inserted, for example, between sections F_i and F_{i+1} in Eq. (1) for a phase shift after the i-th section. This matrix is expressed as

$$F_{\pi} = \begin{bmatrix} \exp\left(\frac{-i\varphi_{i}}{2}\right) & 0\\ 0 & \exp\left(\frac{i\varphi_{i}}{2}\right) \end{bmatrix}, \tag{2}$$

where φ_i represents the shift in phase. The dotted curve of Fig. 1(a) shows the comparison of a simulated spectrum for a phase shift $\varphi = \pi$ with that of a recorded grating with the same shift.

In order to predict the effect of the AOM over the PSFBG [8], the finite element method (FEM) is employed. In this method, the acoustic excitation is taken as

$$s = s_0 e^{iw_{ac}t}, (3)$$

where s_0 is the amplitude of the acoustic wave and $\omega_{\rm ac}$ is the acoustic frequency. The FEM gives the displacement field u(z) along the longitudinal axis (z-axis) of the fiber. Once the displacement field is obtained, the strain field in each one of the finite elements is found by differentiation, as

$$\varepsilon^{e} = \frac{u^{e+1} - u^{e}}{\Delta z},\tag{4}$$

where the index e represents the local nodes and Δz represents the element size in the FEM. The grating spectrum is finally calculated by the TMM with the help of:

$$\Lambda(\varepsilon(z)) = \Lambda_0[1 + (1 - p_e)\varepsilon(z)],\tag{5}$$

where Λ_0 is the pitch when the grating is at rest, p_e is the photoelastic coefficient and $\varepsilon(z)$ is the strain field. The dotted curve of Fig. 1(b) and (c) show the simulated spectra of a PSFBG for acoustic excitations of f= 113 and 621 kHz, respectively, and measured results for the same frequencies. It is noticed that for high frequency excitation, multiple bands appear in the FBG reflection spectrum due to the grating superlattice modulation [4].

3. Experimental procedure

The PSFBG used in the experiments was inscribed in standard single mode photosensitive fiber with the phase mask technique, using a 248 nm KrF laser. The total length of the grating was

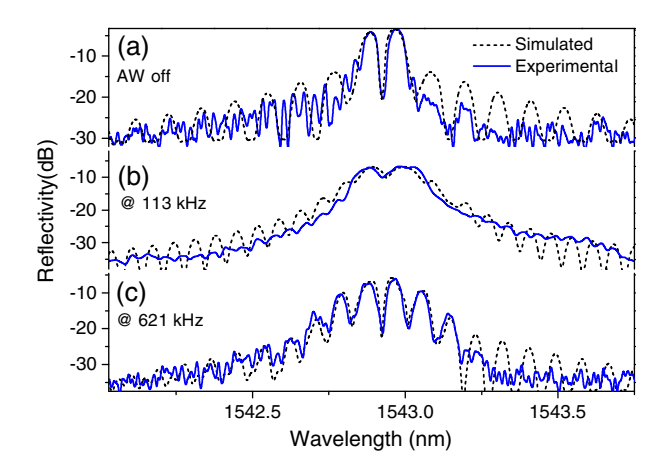


Fig. 1. Simulated (dotted lines) and experimental (solid lines) reflected spectra of a π phase shifted FBG (a) at rest, and when (b) 113 and (c) 621 kHz acoustic wave, at constant PZT load excite the fiber.

 L_g = 25 mm with a phase shift of $\varphi = \pi$ in the middle. An optical network analyzer (resolution = 0.01 nm) was used to characterize properties in the spectral domain.

The experimental set-up is based upon the silica horn-piezo acousto-optic modulator [4], composed by a piezoelectric transducer (PZT), a silica horn and an optical fiber containing the PSFBG. The set-up allows the reflection and transmission spectra to be recorded. This is possible by passing the fiber through the horn and through a hole drilled in the middle of the piezo disc in an arrangement similar to the schematic in Ref. [12]. The silica horn is L_h =50.6 mm, with a base diameter Φ =5 mm, a tip diameter Φ =1 mm and central hole diameter Φ =125.5 µm. Using micron resolution translation stages, the initial tension of the FBG can be adjusted. The acoustic wave interaction length of the horn-fiber set is L_b =95 mm. The set was swept over the range from 1 kHz to 1.3 MHz to investigate the effects on the PSFBG. The end of the fiber is fixed in a holder, which enables the generation of an acoustic standing wave. This way, the acoustic strain field in the grating is stationary.

4. Results

4.1. Notch phase-shift

Fig. 1 shows a comparison of simulated and experimental results when (a) no acoustic wave is applied in the device and when the wave excites the fiber at (b) 113 and at (c) 621 kHz. The results show a good agreement between simulation and experimental data.

Fig. 2(a) and (b) shows, respectively, the reflection and transmission spectra of the PSFBG when the PZT load varies for an acoustic excitation at 113 kHz. Fig. 2(a) shows that the acoustic excitation at 113 kHz leads to a broadening of the PSFBG, which can be controlled with the PZT load. When the load is set at 5 V, the notch is totally suppressed, thus values above that are not considered. Therefore, as the load is increased the notch depth decreases as shown in Fig. 2(a). In the same way, Fig. 2(b) shows the transmission spectra when the PZT load is varied for the same excitation frequency. It is also noticed that the left and right rejection bands depth decrease when the PZT load increases. Indeed, when propagating along the fiber the optical wave sees a change in the optical path, which leads to the destruction of the grating phase matching condition, turning the grating weaker (without coupling to any other mode of the fiber).

On the other hand, it is also possible to control the 3-dB bandwidth of the left and right peaks by adjusting the applied PZT voltage. As the PZT load is increased the side lobes (left and right peak) bandwidth increase as observed in Fig. 2(a). This particular behavior is detailed in Fig. 3. The results show an excellent agreement between left and right peak. In the same way, Fig. 3 also shows that a fine control of the 3-dB bandwidth of left and right rejection bands is achieved by varying the PZT load. In this case, results are presented for PZT loads up to 2.5 V, the maximum measurable 3-dB bandwidth value for the rejection bands. Above this value both bands are suppressed due to the increasing reduction of the grating reflectivity. The results show that the effect is symmetrically observed on both bands.

The notch depth and the rejection band depth can also be changed. It is noticed that the notch depth parameter is linearly dependent on the acoustic intensity for a particular frequency, in this case 113 kHz, as shown in Fig. 4(a). By increasing the PZT load the notch depth can be adjusted from 14 to 0 dB. For higher loads (above 5 V), the notch is completely suppressed, leading to devices that can be implemented using very low voltage sources. Fig. 4(a) shows also a comparison of simulated and experimental data, showing a good agreement between both. Fig. 4(b) shows the simulated and experimental behavior of the rejection band depth. A fine control of the rejection band depth is achieved by varying the PZT load when the wave excite is kept constant.

Download English Version:

https://daneshyari.com/en/article/10641267

Download Persian Version:

https://daneshyari.com/article/10641267

<u>Daneshyari.com</u>